# Increased Usable Frequency Band for Underwater Transducers with Single Crystal

**Røed, Ellen Katrine Sagaas[1, 2]; Andersen, Kenneth Kirkeng[1]; Bring, Martin[2]; Tichy, Frank[2]; Åsjord, Else-Marie[2]; Hoff, Lars[1]**

[1]Department of Microsystems, University of South-Eastern Norway, Horten, Norway
[2]Kongsberg Maritime Sensors and Robotics Horten, Norway

This is an Accepted Manuscript of an article published by IEEE Online in *2020 IEEE International Ultrasonics Symposium (IUS)* on November 17, 2020, available online: https://doi.org/10.1109/IUS46767.2020.9251335

Røed, E. S., Andersen, K. K., Bring, M., Tichy, F., Åsjord, E. -M. & Hoff, L. (2020, September 7-11). Increased Usable Frequency Band for Underwater Transducers with Single Crystal [Conference presentation]. *2020 IEEE International Ultrasonics Symposium (IUS).* Las Vegas, NV. https://doi.org/10.1109/IUS46767.2020.9251335

# Increased Usable Frequency Band for Underwater Transducers with Single Crystal


Ellen Sagaas Røed
*Kongsberg Maritime Sensors and Robotics*
*and*
*University of South-Eastern Norway*
Horten, Norway
ellen.sagaas.roed@km.kongsberg.com

Kenneth Kirkeng Andersen
*Department of microsystems*
*University of South-Eastern Norway*
Horten, Norway
Kenneth.Andersen@usn.no

Martin Bring
*Kongsberg Maritime Sensors and Robotics*
Horten, Norway
martin.bring@km.kongsberg.com

Frank Tichy
*Kongsberg Maritime Sensors and Robotics*
Horten, Norway
frank.tichy@km.kongsberg.com

Else-Marie Åsjord
*Kongsberg Maritime Sensors and Robotics*
Horten, Norway
else-marie.asjord@km.kongsberg.com

Lars Hoff
*Department of microsystems*
*University of South-Eastern Norway*
Horten, Norway
Lars.Hoff@usn.no



***Abstract*— In the increasing market of transducers for small underwater platforms, each transducer should be used for several purposes, hence cover as large frequency range as possible. Bandwidth is commonly defined as the -3 dB limit of the electromechanical transfer function. Many applications can utilize information from the transducer far beyond this limit. However, another relevant restriction for underwater transducers confined in a small space is the maximum reactive power, limited by the heating and size of electronic components. The higher electromechanical coupling factors of piezoelectric single crystals compared to PZTs enable a wider frequency band with acceptable electrical power factor. In this paper we use a 1D model to find the usable frequency band for two water loaded 1-3 composite transducers, restricted by electrical power factor > 0.5 and electromechanical transfer function > -12 dB. The transducers have air backing and three numerically optimized matching layers. One transducer has PZT as the active material. The effective electromechanical coupling factor of this transducer is 0.69 and the usable bandwidth is calculated to 120 %, referred to the center of the band. The second transducer has single crystal as the active material and an effective electromechanical coupling factor of 0.87. For the single crystal transducer, the usable bandwidth is calculated to 150 %.**



**Keywords—single crystal, matching layer, 1-3 composite**


## I. Introduction

Ocean science is in the middle of a robotic revolution, with small platforms that can gather information from places and at times that was previously not accessible. The ultrasonic transducers placed on the small platforms should be as compact as possible. Each transducer should preferably be used for several purposes, hence cover as large frequency range as possible. The more frequencies available for data collection, the more detailed information is provided.

Single crystals in the relaxor-ferroelectric lead magnesium niobate (PMN)-lead titanate (PT) system provide advantages over conventional lead zirconate titanate (PZT) ceramics when used as the active material in piezoelectric transducers. PMN-PT single crystals have superior piezoelectric coefficients and electromechanical coupling coefficients to PZT, offering potential for larger acoustic source levels and broader frequency bandwidth [1][2]. PMN-PT has become a widely used material in high-end medical transducers, but its high cost per unit volume has limited its use in underwater transducers. The robotic revolution has however renewed the interest for single crystals in underwater transducers, as the single crystals provide a unique opportunity for equipping a small robot with more frequencies. Both the large piezoelectric coefficients and the large mechanical compliance compared to PZT are advantageous for compact design. In addition, the superior electromechanical coefficients provide acceptable electrical impedance phase over a wide frequency range [3], enabling high power transmission without damaging small electronic components, even at frequencies far from the resonance frequency. This can possibly reduce the number of transducers required for a given mission, which is the motivation behind the comparison of usable frequency bands presented in this work.


Funded by the Research Council of Norway, Grant no. 290462


## II. Definition of useable frequency band

One definition of conventional bandwidth is based on the electromechanical transfer function *H(f)*,

$$H(f) = \frac{u(f)}{V(f)}, \tag{1}$$

where *f* is the frequency, *u(f)* is the normal velocity at the face of the transducer, and *V(f)* is the voltage at the electrical terminal of the transducer. The conventional transfer function bandwidth is the range of frequencies where

$$20\ \log_{10}\frac{|H(f)|}{|H(f_0)|} \geq -3\ dB\ , \tag{2}$$

with $f_0$ being the frequency where the transfer function *H(f)* has its maximum value.

However, many underwater applications can utilize information from the transducer far beyond this limit. Narrowband pulses can be generated from different sub-bands, to collect different kinds of information. Low frequencies can be used for long range, and high frequencies for high resolution. When the transducer is used in this way, a total transfer function variation smaller than – 3 dB is of less importance. However, the transfer function will still impose limitations on the usable frequency band, mainly due to the dynamic range of the electronics. The dynamic range varies from application to application, but in this work the useable frequency band is restricted by:

$$20\ \log_{10}\frac{|H(f)|}{|H(f_0)|} \geq -12\ dB. \quad (3)$$

This is a relaxed restriction on the transfer function, but another limit for the usable frequency band is imposed by the reactive electrical power. In the confined space of a small robot, the electronic components need to be small. If the reactive power is too large, dissipation in the electronics will cause overheating. The power, *P*, used to drive a transducer consists of a real part, $|P|\cos\theta$, and a reactive part, $|P|\sin\theta$, where $\theta$ is the phase of the transducer's electrical impedance. The factor $\cos\theta$ is called the electrical power factor, *PF*, given by:

$$PF = \cos\theta. \quad (4)$$

In this work, to keep the reactive power at an acceptable level and avoid overheating, the usable frequency band is limited to the frequency range where

$$PF > 0.5. \quad (5)$$

This corresponds to an absolute electrical phase smaller than 60°. To ensure effective operation of the transducer, the capacitive part of the electrical impedance is tuned out at resonance. The phase relevant for the reactive power is the phase after tuning.

In a previous study [4], we optimized bandwidth for a single crystal transducer, using a definition of bandwidth similar to Stansfield's [5], requiring the transfer function to be larger than -3 dB and the power factor to be larger than 0.8. We saw then that a large part of the frequency band between the outer flanks of the power factor was left unutilized.

In the present study, we look at the potential of single crystals in applications where a more relaxed bandwidth definition can be accepted. To summarize, the total usable frequency bandwidth in the present study is defined as the range of frequencies where the transfer function is within -12 dB of its maximum value, and where the electrical phase after tuning is within ±60º, i.e. power factor > 0.5.

## III. The Transducers

The usable frequency bandwidth is compared for two transducers, schematically illustrated in fig. 1 The transducers

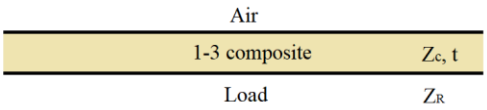


Fig. 1. The transducers are made from 1-3 composite plates vibrating in the thickness mode. The composites have 50% volume fraction PZT5A or PIN-PMN-33%PT in a matrix of soft epoxy. The backing is air.

TABLE I. Effective Composite Parameters

| **Parameter** | **Symbol (unit)** | **PIN-PMN-33%PT composite** | **PZT5A composite** |
|---|---|---|---|
| Piezoelectric constant | $h_{33}$ ($10^8$V/m) | 28.6 | 25.8 |
| Electrical permittivity | $\varepsilon_{33}^S$ ($\varepsilon_0$) | 467 | 433 |
| Acoustic impedance (open circuit) | $Z_c$ (MRayl) | 14 | 15 |
| Acoustic impedance (short circuit) | $Z_{cs}$ (MRayl) | 7 | 11 |
| Longitudinal velocity | $v^D$ (m/s) | 3200 | 3591 |
| Electromechanical coupling coefficient | $k_t$ | 0.87 | 0.69 |
| Mechanical quality factor | $Q_m$ | 40 | 40 |

are made from 1-3 composite plates vibrating in the thickness mode. One composite plate consists of PZT5A and soft epoxy, with 50% volume fraction PZT. The other composite plate consists of single crystal PIN-PMN-33%PT and soft epoxy, with 50% volume fraction single crystal. The composites have air backing. The effective material parameters of the composites are calculated in accordance with [6] and given in Table I. Note that the PZT composite has effective electromechanical coupling coefficient $k_t$=0.69, while the single crystal composite has $k_t$=0.87.

## IV. Frequency Independent Perfect Matching

The bandwidths of the transfer function and the power factor depend on both the electromechanical coupling coefficient and the degree of matching between the acoustic impedances of the transducer and its loading. As an initial illustration, we study the case of frequency independent perfect matching, meaning that the short circuit acoustic impedance of the transducer is equal to the acoustic impedance of the load, at all frequencies. The back port is air loaded. The front load, $Z_R$, is considered real. Using the 1D distributed Mason model, the transfer function for a piezoelectric plate in the thickness mode can then be written:

$$H(f) = \frac{1}{NZ_R}\frac{1}{\left[1-\frac{1}{2(\sin x)^2}+\frac{k^2\cos x}{2x\sin x}\right]+j\left[\frac{Z_c}{Z_R}\left(\frac{\sin x}{\cos x}\right)-\frac{1}{\sin x\cos x}+\frac{k^2}{x}\right]} \quad (6)$$

where $x = (\omega t)/(2v^D)$, with $\omega$ being the angular frequency $2\pi f$, $t$ being the plate thickness and $v^D$ being the longitudinal

wave velocity $v^D = \sqrt{c_{33}^D/\rho}$. The velocity is expressed by density ρ and the open circuit stiffness coefficient $c_{33}^D$. $N$ is the transformation ratio of the Mason model. We have used

$$\frac{N^2}{\omega C_0 Z_C} = \frac{\varepsilon_{33}^S A^2 c_{33}^D k_t^2 t}{t^2 \omega \varepsilon_{33}^S A \rho v^D A} = \frac{k_t^2}{2x} \quad (7)$$

to simplify the expression. Here $C_0$ and $\varepsilon_{33}^S$ are the clamped capacity and permittivity and $Z_c$ is the open circuit acoustic impedance of the transducer, $Z_c = A\rho v^D$. The area, $A$, of the transducer is set equal to the area of the load. The factor $1/NZ_R$ is frequency independent and will disappear when the transfer function is normalized.

Fig. 2 shows the magnitude of the transfer function for frequency independent perfect matching for transducers with coupling factors $k_t$=0.69 and $k_t$=0.87.

The influence of $k_t$ on the transfer function could be easily identified in the 1D distributed Mason model. This is not so straightforward for the power factor. However, a lumped model expression for the power factor is given in [7] as:

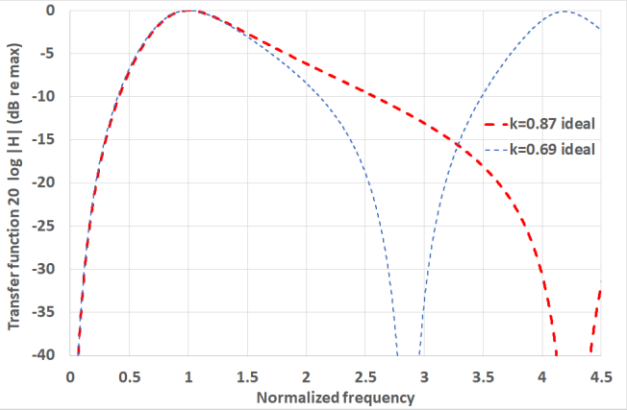


Fig. 2. Normalized electromechanical transfer function for the ideal case of frequency independent perfect matching. The frequency axis is normalized to resonance. Red, thick line: transducer with $k_t$=0.87. Blue, thin line: transducer with $k_t$=0.69.

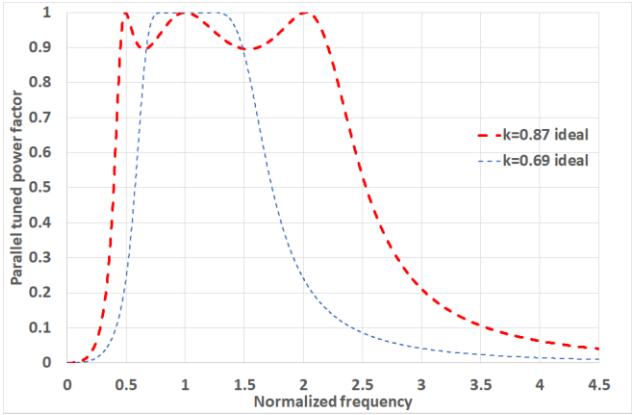


Fig.3. Parallel tuned electrical power factor for the ideal case of frequency independent perfect matching. The frequency axis is normalized to resonance. Red, thick line: transducer with $k_t$=0.87. Blue, thin line: transducer with $k_t$=0.69.

$$PF = \cos\theta = 1/\sqrt{1+\tan\theta} \quad (8)$$

$$\tan\theta = \left[\frac{1-k^2}{Q_m k^2} - Q_m + \frac{1-k^2}{k^2} Q_m \left(\frac{\omega}{\omega_r} - \frac{\omega_r}{\omega}\right)^2\right]\left(\frac{\omega}{\omega_r} - \frac{\omega_r}{\omega}\right) \quad (9)$$

The last expression is for a transducer where the clamped capacitance is tuned out by a parallel inductor. The mechanical quality factor, $Q_m$, is the inverse of the – 3 dB bandwidth of the transfer function and can be extracted from Fig. 2. The power factor for frequency independent perfect matching is then given by $k_t$ only, and is shown for $k_t$=0.69 and $k_t$=0.87 in Fig. 3.

We see from Fig. 2 and Fig. 3 that the higher $k_t$ gives a wider frequency band with $PF$>0.5. For $k_t$=0.87 this power factor bandwidth is much larger than the conventional -3 dB transfer function bandwidth. However, when allowing the transfer function to drop -12 dB, the useable bandwidth will be limited by the power factor, not the transfer function magnitude. For frequency independent perfect matching, the fractional power factor bandwidth is 100 % for $k_t$=0.69 and 150 % for $k_t$=0.87, referred to the center of the band. Note that the center of the band is shifted up from resonance. For $k_t$=0.87 this means that the fractional bandwidth will be significantly larger if instead referred to resonance.

## V. Optimization of Frequency Dependent Matching Layers

In real composite transducers, matching is often obtained by adding quarter wavelength matching layers. Guidelines for the acoustic impedances of the layers is given e.g. by DeSilets et al. [8]. We now add three matching layers to our transducers, see fig. 4. The matching layers do not provide frequency independent matching. On the contrary, they introduce strong frequency dependence. When optimizing bandwidth for the two example transducers, we therefore use a full distributed model that includes the distributed terms for the matching layers, not reducing them to frequency independent loads.

We optimize usable bandwidth under the definition given in section II, i.e. transfer function magnitude > -12 dB (3) and power factor > 0.5 (5), using a gradient-based numerical algorithm implemented in MATLAB's *Global Optimization Toolbox*, as previously described for a different set of optimization criteria [9]. The air-backed and water-loaded transducers are modelled by the one-dimensional distributed Mason model, including three acoustic matching layers. The electrical impedance and the electromechanical transfer function are calculated for various matching layer thicknesses and acoustic impedances. The electrical impedance phase is tuned to zero at the resonance frequency by a parallel inductor, and the tuned electrical phase is used to calculate the tuned

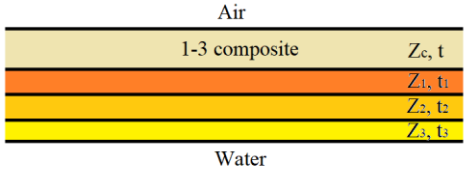


Fig. 4. Three acoustic matching layers added to the transducer.

power factor. Usable bandwidth, $\Delta f$, is calculated referred to the bandwidth center. The optimization algorithm is run to minimize a cost function $E=1/\Delta f$. The parameters to be optimized are acoustic impedances and thicknesses for the inner ($Z_1$,$t_1$), middle ($Z_2$,$t_2$) and outer matching layers ($Z_3$,$t_3$), with the parameter range for the run given in table II.

## VI. Results and Discussion

The results from the optimization are shown in Fig. 5. We found that with three acoustic matching layers, an increase in coupling coefficient from $k_t$=0.69 to $k_t$=0.87 does give a considerable bandwidth improvement, using the definition given in (3) and (5). The ripple within the band is however larger than for frequency independent perfect matching. The usable bandwidth for the single crystal transducer is approximately equal to the ideal case, 150 % referred to the bandwidth center. For the PZT composite, the useable band is now centered around resonance and have a width of 120 %. For $k_t$=0.87, the transfer function is now limiting the bandwidth. This demonstrates that even with the limit for the transfer function magnitude set as low as -12 dB, it is difficult to achieve an acoustic impedance matching good enough to utilize the full power factor bandwidth of the high coupling single crystals. The acoustic impedances and matching layer thicknesses resulting from the optimization are shown in Table III.

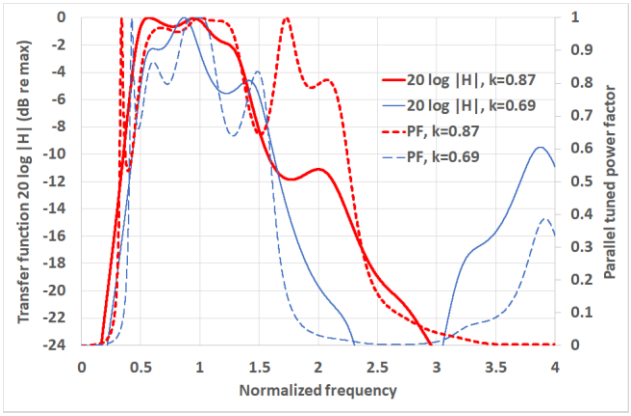


Fig.5. Electromechanical transfer function (solid lines) and parallel tuned electrical power factor (dashed lines) after numerical optimization of useable bandwidth for transducers with three matching layers. The frequency axis is normalized to the resonance frequency. Red, thick lines: transducer with $k_t$=0.87. Blue, thin lines: transducer with $k_t$=0.69.

TABLE II PARAMETER RANGE FOR THE OPTIMIZATION

| Parameter | Start value[a] | Minimum value | Maximum value |
|---|---|---|---|
| $Z_1$ | 7.7 MRayls | 3.16 MRayls | 1.75 MRayls |
| $Z_2$ | 5 MRayls | 2 MRayls | 1.5 MRayls |
| $Z_3$ | 9 MRayls | 4.2 MRayls | 2.2 Mrayls |
| $t_1$ | 0.25λ[b] | 0.1λ | 0.4λ |
| $t_2$ | 0.25λ | 0.1λ | 0.4λ |
| $t_3$ | 0.25λ | 0.1λ | 0.4λ |

[a] Start values according to [8] for $Z_c$=14.

[b] λ=wavelength at resonance.

TABLE III OPTIMUM PARAMETERS FOUND

| Parameter | Optimized value, $k_t$=0.87 | Optimized value, $k_t$=0.69 |
|---|---|---|
| $Z_1$ | 7.19 MRayls | 8.8 MRayls |
| $Z_2$ | 3.55 MRayls | 4.08 MRayls |
| $Z_3$ | 1.91 MRayls | 1.80 MRayls |
| $t_1$ | 0.38λ | 0.24λ |
| $t_2$ | 0.26λ | 0.30λ |
| $t_3$ | 0.37λ | 0.19λ |

## VII. Conclusions

Single crystals have larger electromechanical coupling coefficients than PZT. A larger coupling coefficient provides potential for a larger frequency band with power factor > 0.5. For an air-backed piezoelectric plate that is perfectly matched to the front load at all frequencies, the power factor bandwidth, referred to the center of the band, is 150 % for $k_t$=0.87 compared to 100% for $k_t$=0.69. This increase of power factor bandwidth is advantageous in transducers mounted on small underwater platforms, as it allows the transducers to be used in a wider frequency range without risk of the reactive power damaging small electronic components. When this is fulfilled, many transducers can be used outside the conventional -3 dB transfer function bandwidth. In this work, the transfer function is allowed to drop -12 dB.

In a practical transducer, acoustic matching is obtained by adding frequency dependent matching layers to the transducer. Numerical optimization of three acoustic matching layers shows that even with three layers, imperfect acoustic matching causes a narrowing of the transfer function bandwidth for the example transducer with $k_t$=0.87. However, a usable bandwidth close to the case of perfect matching is achievable, if large ripple within the band is tolerated.

## References


[1] L. M. Ewart, E. A. McLaughlin, H. C. Robinson, J. J. Stace and A. Amin, "Mechanical and electromechanical properties of PMNT single crystals for naval sonar transducers," IEEE Trans. Ultrason., Ferroelectr., Freq. Contr., vol. 54, no. 12, pp. 2469-2473, 2007.

[2] N. P. Sherlock and R. J. J. Meyer, "Modified single crystals for high-power underwater projectors," IEEE Trans. Ultrason., Ferroelectr., Freq. Contr., vol. 59, no. 6, pp. 1285-1291, 2012.

[3] H. C. Robinson, R. Janus, J. O'Neal, C. Mattews, J. Chace and J. Moore, "Low frequency range tracking transducer," in OCEANS MTS/IEEE, Monterey, 2016.

[4] E. S. Røed, K. K. Andersen, M. Bring, F. Tichy, E-M. Åsjord and L. Hoff, "Acoustic impedance matching of PMN-PT/epoxy 1-3 composite transducers with usable bandwidth restricted by electrical power factor", in IEEE Int. Ultrason. Symp, Glasgow, 2019.

[5] D. Stansfield, Underwater Electroacoustic Transducers, Bath, UK: Bath University Press, 1991.

[6] W. A. Smith and B. A. Auld, "Modeling 1-3 composite piezoelectrics: Thickness-mode oscillations," IEEE Transactions on Ultrasonics, Ferroelectrics and Frequency Control, vol. 38, no. 1, pp. 40-47, 1991.

[7] C. H. Sherman and J. L. Butler, Transducers and Arrays for Underwater Sound, New York: Springer, 2007.

[8] C. S. DeSilets, J. D. Fraser and G. S. Kino, "The design of efficient broad-band piezoelectric transducers," IEEE Trans. Sonics Ultrason., Vols. SU-25, no. 3, pp. 115-125, 1978.

[9] K. K. Andersen, M. E. Frijlink and L. Hoff, "A numerical optimization method for transducer transfer functions by the linearity of the phase spectrum," IEEE Trans. Ultrason., Ferroelectr., Freq. Contr., vol. 66, no. 1, pp. 71-78, 2019.